

# The distribution of oblique reflection energy in the prestack volume $V(x, h, t)$ .

John C. Bancroft and Charles P. Ursenbach, University of Calgary / CREWES



## Abstract

The travel-time surface that is defined by the reflections from an oblique reflector is defined. Knowledge of this surface enables an accurate prestack Kirchhoff migration of oblique reflection energy, and aids in defining an optimum method of stacking prior to poststack migration.

## Introduction

Seismic lines are usually designed with an orientation that is normal to the geological structure or in the dip direction. With this orientation, all reflections are confined to the vertical plane below the seismic line. Occasionally, some reflecting surface are oblique to the seismic line, with their reflection points beyond the vertical plane as illustrated in Figure 1. French (1975) showed that the zero-offset reflection energy that comes from beyond the vertical plane (Figure 1a) may be used to help image the area where the oblique reflector crosses the vertical plane. This poststack procedure is accomplished by increasing the migration velocity  $V_{mig}$  by

$$V_{mig} = \frac{V_{ms}}{\cos\gamma}, \quad (1)$$

where  $V_{ms}$  is the RMS velocity and  $\gamma$  is the angle of obliquity. However, only that portion of the migrated section that contains the oblique reflectors will be imaged correctly.

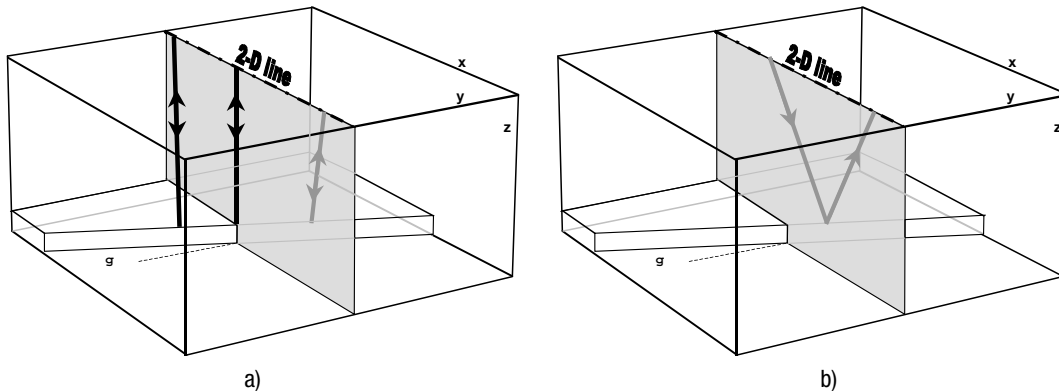


Figure 1 Perspective view of a 2-D seismic line above an oblique reflector, a) for the zero-offset case, and b) for the offset case.

## Prestack traveltimes

Reflections from offset data also come from reflection points that are beyond the vertical plane as illustrated in Figure 1b. When the reflectors are normal to the 2-D line, the prestack reflection points are also in the vertical plane and the traveltimes are easily defined by double square root (DSR) equation. The prestack traveltimes from oblique reflection are not defined by the DSR equation, but are defined by a more complex equation that is presented below.

Consider the plan view of the oblique reflector in Figure 2a. Note the location **A** where the oblique reflector intersects vertical plane below the seismic line. The CMP gather at **A** contains symmetric source-receiver locations (identified by the square braces) and all raypaths will also be in the vertical plane. For this case only, the moveout on the offset traces will be hyperbolic with an RMS velocity that is typically associated with a normal reflector.

The reflection points for a CMP gather located at **B** will be considerably different from the reflections points at **A**. At **B**, the zero offset reflection has a migration velocity  $V_{mig}$  defined in equation (1). Small offsets from B will have a reflection point that is close to the zero offset point and may appear to have a moveout velocity close to  $V_{mig}$ . For larger offsets, the reflector point  $(x_p, y_p)$  will move along the reflector towards A.

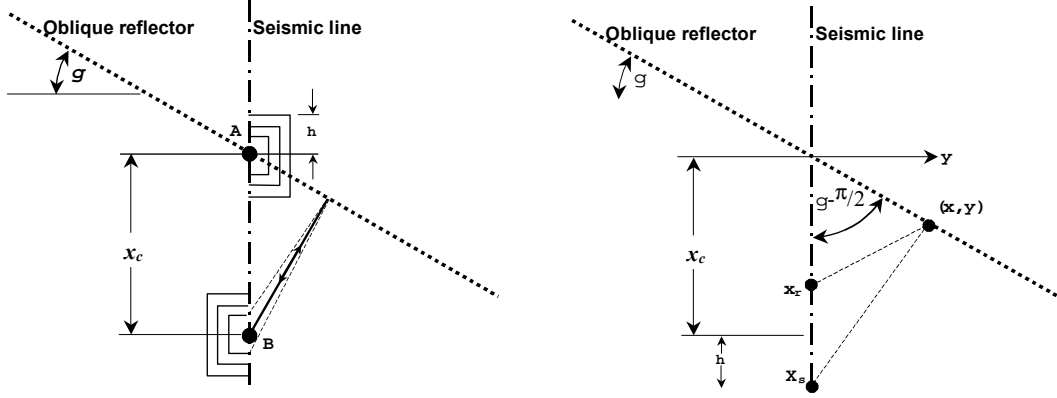


Figure 2 Plan view of an oblique reflector showing a) CMP gathers at A and B, and b) the geometry for computing the point of reflection.

Let the source location is defined by  $(x_s, y_s = 0, z_s = 0)$ , the receiver location by  $(x_r, y_r = 0, z_r = 0)$ , the reflection point on the oblique line be  $(x, y, z=1)$ , the angle of obliquity  $\gamma$ , and the relative slope of the reflector in the  $x$ - $y$  plane be defined by  $m = \tan(\gamma - \pi/2)$ .

The total length of the raypath  $l$  is for any point on the reflector  $(x, y)$  is

$$l = \left[ (x_s - x)^2 + y^2 + z^2 \right]^{1/2} + \left[ (x_r - x)^2 + y^2 + z^2 \right]^{1/2} \quad (2)$$

Replacing the  $y$  parameter in equation (2) with  $x$  is accomplished by using the linear equation  $y = mx$  giving

$$l = \left[ (x_s - x)^2 + m^2 x^2 + z^2 \right]^{1/2} + \left[ (x_r - x)^2 + m^2 x^2 + z^2 \right]^{1/2} \quad (3)$$

In accordance with Fermat's principle, the minimum length of the raypath  $l$  will define the location of the reflection point  $(x_p, y_p)$ . Consequently, taking the derivative of equation (3) with respect to  $x$  and equating it to zero will define  $x_p$ , i.e.

$$\frac{dl}{dx} = \frac{2m^2 x - 2(1-x)}{2\sqrt{m^2 x^2 + (x_s - x)^2 + z^2}} + \frac{2m^2 x - 2(2-x)}{2\sqrt{m^2 x^2 + (x_r - x)^2 + z^2}} = 0 \quad (4)$$

The solution for  $x_p$  was found to be

$$\left\{ x_p \frac{-z \cdot m^2 (x_r x_s - z^2) + \sqrt{z^2 + m^2 (x_r^2 + z^2)} \sqrt{z^2 + m^2 (x_s^2 + z^2)}}{m^2 (1 + m^2) (x_r + x_s)} \right\} \quad (5)$$

and the value of  $y_p$  is obtained from the linear equation  $y = mx$ . The value of  $x_p$  is then inserted into equation (3) to give the total length of the ray-path  $l$  as defined in equation (6).

$$l = \sqrt{\left\{ z^2 + \frac{1}{4 m^2 (1 + m^2)^2 x^2} \left( (-z^2 + m^2 ((-h + x)(h + x) - z^2) + \sqrt{z^2 + m^2 ((-h + x)^2 + z^2)} \sqrt{z^2 + m^2 ((h + x)^2 + z^2)} \right)^2 \right\}} + \sqrt{\left\{ z^2 + \frac{1}{4 m^2 (1 + m^2)^2 x^2} \left( (-z^2 + m^2 ((-h + x)(h + x) - z^2) + \sqrt{z^2 + m^2 ((-h + x)^2 + z^2)} \sqrt{z^2 + m^2 ((h + x)^2 + z^2)} \right)^2 \right\}} + \sqrt{\left\{ z^2 + \frac{1}{4 m^2 (1 + m^2)^2 x^2} \left( (-z^2 + m^2 ((-h + x)(h + x) - z^2) + \sqrt{z^2 + m^2 ((-h + x)^2 + z^2)} \sqrt{z^2 + m^2 ((h + x)^2 + z^2)} \right)^2 \right\}} + \sqrt{\left\{ z^2 + \frac{1}{4 m^2 (1 + m^2)^2 x^2} \left( (-z^2 + m^2 ((-h + x)(h + x) - z^2) + \sqrt{z^2 + m^2 ((-h + x)^2 + z^2)} \sqrt{z^2 + m^2 ((h + x)^2 + z^2)} \right)^2 \right\}} \quad (6)$$

To view the traveltime surface, a model was designed with a constant velocity of unity ( $V = 1$ ) allowing the traveltimes to be estimated as distance. The depth of the scatterpoint was located at a depth  $z = 1$ , with the maximum displacement and offset of  $x_c = h = 4$ . The traveltime surface for reflections from the oblique reflector for continuous CMP locations  $x_c$  and offsets  $h$ , is shown in Figure 3a. The traveltime surface for a normal reflector ( $\alpha=0$ ) at A is referred to as Cheops pyramid and shown in Figure 3b for comparison.

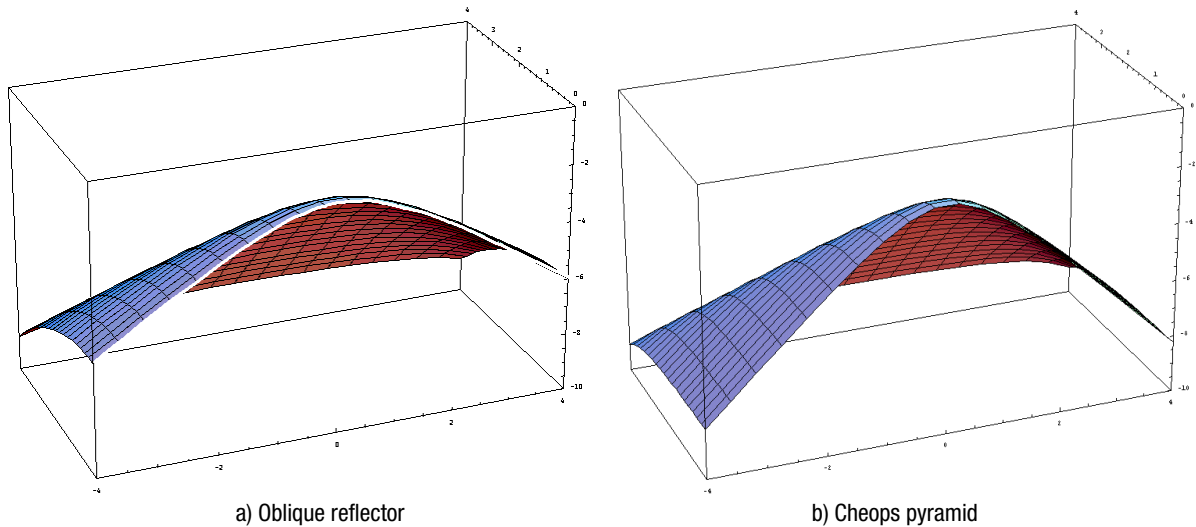


Figure 3 Reflection times in the prestack volumes  $(x, h, t)$  for a) an oblique reflector, and b) Cheops pyramid for a normal reflector.

Note in Figure 3, the difference in the zero offset hyperbolas defined by  $V_{mig}$  for the oblique reflector and  $V_{ms}$  for the normal reflector. The offset curvatures through the peaks are the same and have a moveout velocity  $V_{ms}$ . The moveout at maximum displacement  $x_{c-max}$  can be observed at the left side of each figure. Note the Cheops pyramid moveout is quite flat (especially near zero offset) and requires a moveout velocity that is modified by the corresponding dip on the zero offset diffraction. The corresponding moveout on the oblique reflector surface (ORS) appears more hyperbolic and with a lower velocity.

Similar traveltime surfaces for conventional processing (NMO and poststack migration) may be compared with these surfaces. Two prestack surfaces using NMO correction velocities  $V_{ms}$  and  $V_{mig}$  are shown with front and rear views in Figure 4. For an easier comparison, the oblique reflecting surface is also plotted in each figure. In the Figure 4a, the ORS is always above the  $V_{ms}$  surface, while in Figure 4b, the ORS is always below the  $V_{mig}$  surface.

**Comments**

Offset data requires special consideration, as it will not stack exactly to the zero offset hyperbola. Note that using an RMS velocity for NMO correction does provide an exact fix at small  $x$  displacements and a reasonable fit at small offsets, producing reasonable results with a standard processing flow. Choosing  $V_{mig}$  as the NMO correction velocity will produce considerably more error and is not recommended.

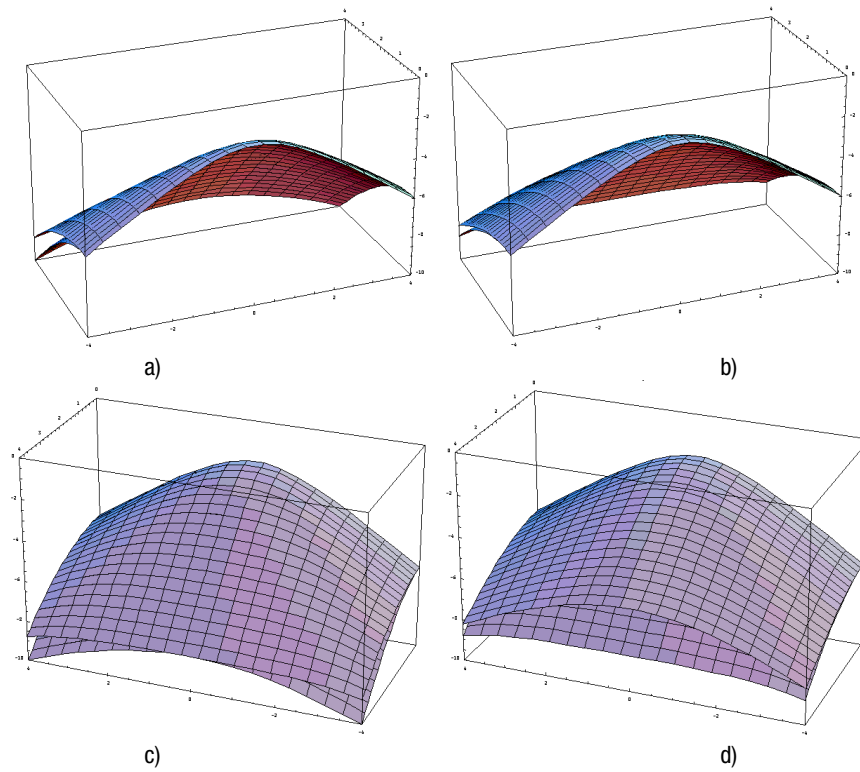


Figure 4 Combined plots of the oblique reflector surface with a) conventional moveout, and b) with moveout velocities using  $V_{mig}$  defined in equation (1). The rear view of (a) and (b) are shown in parts (c) and (d) respectively.

**Conclusions**

The prestack migration traveltime surface of oblique reflectors may be defined exactly (with RMS velocity assumptions). Conventional stacking with RMS velocities also provides a reasonable solution.

**References**

French, W. S., 1975, Computer migration of oblique seismic reflection profiles, *Geophysics*, 40. 961-980  
 Bancroft, J. C., and Ursenbach, C. P., 2000, Prestack considerations for the migration of oblique reflectors, CREWES Research Report, p 461-467